Alterations in extracellular matrix composition during aging and photoaging of the skin

Maxwell C. McCabe[a], **Ryan C. Hill**[a], **Kenneth Calderone**[b], **Yilei Cui**[b], **Yan Yan**[b], **Taihao Quan**[b], **Gary J. Fisher**[b] **and Kirk C. Hansen**[a]

***a* - Department of Biochemistry and Molecular Genetics,** *School of Medicine, University of Colorado, 12801 E 17th Ave., Aurora, CO 80045, USA*
***b* - Department of Dermatology,** *University of Michigan, 1150 W. Medical Center Drive, Medical Science I R6447, Ann Arbor, MI 48109, USA*

Correspondence to Kirk C. Hansen: *kirk.hansen@cuanschutz.edu.*
https://doi.org/10.1016/j.mbplus.2020.100041

Abstract

Human skin is composed of the cell-rich epidermis, the extracellular matrix (ECM) rich dermis, and the hypodermis. Within the dermis, a dense network of ECM proteins provides structural support to the skin and regulates a wide variety of signaling pathways which govern cell proliferation and other critical processes. Both intrinsic aging, which occurs steadily over time, and extrinsic aging (photoaging), which occurs as a result of external insults such as solar radiation, cause alterations to the dermal ECM. In this study, we utilized both quantitative and global proteomics, alongside single harmonic generation (SHG) and two-photon autofluorescence (TPAF) imaging, to assess changes in dermal composition during intrinsic and extrinsic aging. We find that both intrinsic and extrinsic aging result in significant decreases in ECM-supporting proteoglycans and structural ECM integrity, evidenced by decreasing collagen abundance and increasing fibril fragmentation. Intrinsic aging also produces changes distinct from those produced by photoaging, including reductions in elastic fiber and crosslinking enzyme abundance. In contrast, photoaging is primarily defined by increases in elastic fiber-associated protein and pro-inflammatory proteases. Changes associated with photoaging are evident even in young (mid 20s) sun-exposed forearm skin, indicating that proteomic evidence of photoaging is present decades prior to clinical signs of photoaging. GO term enrichment revealed that both intrinsic aging and photoaging share common features of chronic inflammation. The proteomic data has been deposited to the ProteomeXchange Consortium via the PRIDE partner repository with the data set identifier PXD015982.

Introduction

Human skin is composed of a dense array of extracellular matrix (ECM) proteins, which are essential for the organ's structural and mechanical properties as well as functions [1]. The collagen-rich ECM is an essential component of dermal vasculature, structural support, and overlying epidermis hemostasis. While all organs change over time as a result of the natural aging process, changes due to aging in skin are exacerbated by a number of environmental factors, including exposure to ultraviolet (UV) radiation [2] and micro-organisms [3]. Cutaneous aging can be classified into natural aging, also known as intrinsic aging, and photoaging, also known as extrinsic aging [4,5]. Histological and ultrastructural studies have revealed that the major alterations in both intrinsically aged and photoaged skin are localized in the connective tissue dermis [6] and to a much lesser extent the cornified envelope (CE) [7]. Biochemical evidence indicates that the prominent molecular features of intrinsic aging in skin are fragmentation of collagen fibrils and declined collagen synthesis [8,9]. Since

collagen fibrils are responsible for much of the strength and resiliency of skin, their degeneration with aging causes skin to become fragile and easily bruised [10,11]. Age-related dermal ECM alterations impair skin dermis structural and mechanical properties and create a tissue microenvironment that promotes age-related skin diseases, such as thinning [12], increased fragility [10], impaired vasculature support [13,14], and poor wound healing [15]. Additionally, aging and sun exposure are two of the most significant risk factors for development of skin cancers [16]. In addition to the known increase in genetic alterations found in aged skin, the stromal microenvironment is altered and can promote tumorigenesis [17]. As such, characterization of skin, including the collagen-rich ECM, is of considerable interest.

The primary objectives of this work are to characterize the skin proteome with a focus on matrisomal proteins that are altered between young and aged human skin as well as between sun-exposed and sun- protected skin. The matrisome [18] is composed of a large number of heterogeneous ECM components and proteins that modify and interact with the ECM. The original matrisome [18] contains soluble factors with limited data to support direct sequestration to the ECM and lacks Cell-ECM receptors and GAG modifying enzymes, demonstrating the need for a more specific definition of proteins which genuinely compose the ECM. The matrisome is composed of two groups: the core matrisome (consisting of collagens, ECM glycoproteins and proteoglycans) and matrisome-associated proteins (consisting of ECM-affiliated proteins, ECM regulators, and secreted factors). Moreover, alterations that occur in aged, as well as sun-exposed, skin have not been characterized in detail. A recent review of previously published skin proteomes found significant disparities between the data presented by different groups, with only 56 consensus proteins appearing in the reviewed databases [19]. Among proteins that were not consistently identified in all skin proteomes were collagen I and elastin, two of the most abundant proteins in human skin, highlighting the poor coverage of more insoluble skin components. Additionally, each of the proteomic data sets ascribe only 2–3% of total protein signal from skin to ECM proteins, drastically underrepresenting the ECM as a fraction of total protein content [19]. Our method generates improved coverage of inaccessible ECM proteins, allowing us to obtain a deeper molecular-level characterization of extracellular matrix alterations within the skin during aging than has been possible with previous techniques. In this study, we obtained full-thickness skin biopsies from young (mean age 26.7 ± 1.3 years) and aged (mean age 84.0 ± 1.7 years) subjects at three anatomical locations representing three levels of photoexposure: hip, underarm, and forearm. We then analyzed these samples for dermal alterations during the processes of intrinsic and extrinsic aging using single harmonic generation (SHG) and two-photon autofluorescence imaging (TPAF) alongside global and quantitative proteomics.

Materials and methods

Procurement of human skin samples

Skin biopsies were obtained from clinically normal adult Caucasian volunteers with no history of skin inflammatory conditions or chronic diseases such as diabetes; 22–30 years for young group (mean age 26.7 ± 1.3 years, males n = 2; females n = 4) and 80+ years for aged group (mean age 84.0 ± 1.7 years, males n = 2; females n = 4). For global proteomics, 3 subjects from young (males n = 1; females n = 2) and aged (females n = 3) sample groups were used for analysis. Three punch biopsies (hip, forearm, and underarm) were obtained from each subject. Photodamage of dorsal forearm skin was judged by wrinkles, pigmentation, skin turgor, and subject history of sun exposure [20]. Full thickness skin samples were 4 mm in diameter. All procedures involving human subjects were approved by the University of Michigan Institutional Review Board, and all subjects provided written informed consent before entering the study.

Second-harmonic generation (SHG) microscopy

For second harmonic generation microscopy, skin sections (100 μm) were fixed with 2% paraformaldehyde for 30 min, and SHG images were obtained using a Leica SP8 Confocal Microscope with 2-Photon (University of Michigan Microscopy and Image Analysis Laboratory), as described previously [21].

CT-FIRE [22] with default parameters was used to extract collagen fiber lengths and widths from SHG image stacks. 10 slices were selected evenly from each image stack for analysis.

Sample preparation for LC-MS/MS

Skin samples were processed as previously described [23]. Briefly, fresh frozen samples were milled in liquid nitrogen with a mortar and pestle. Approximately 5 mg of each sample was processed by a step-wise extraction resulting in cellular, soluble ECM (sECM), and insoluble ECM (iECM) fractions for each sample [24]. Optimized for the skin samples, 3 mm glass beads were used to mechanically agitate samples in a NextAdvance Bullet Blender prior to all cellular and sECM extraction steps. Protein concentration of each fraction for each sample was carried out by A660 Protein Assay

(Pierce™). Proteolytic digestion was carried out according to the FASP protocol [25] with 10 kDa molecular weight cutoff filters. Samples were prepared for 5 LC-MS/MS injections. Approximately 30 µg of protein from each fraction was combined with 500 fmol of stable isotope labeled quantitative concatemers (QconCATs [26]) representing ECM, ECM-associated, and cellular proteins of interest [27]. Samples were reduced, alkylated, and digested with trypsin at 37 °C for 14 h. Peptides were recovered from the filter using successive washes of 50 mM ammonium bicarbonate and 0.1% formic acid. Final volume was adjusted to inject 6 µg of protein and 100 fmol of QconCAT standard for each run.

Mass spectrometry

Global proteomics was carried out (n = 3 per group) on an LTQ Orbitrap Velos mass spectrometer (Thermo Fisher Scientific) coupled to an Eksigent nanoLC-2D system through a nanoelectrospray LC–MS interface. Sixteen µL of each sample was injected into a 20 µL loop using the autosampler. Peptides were desalted on a trapping column (ZORBAX 300SB-C18, dimensions 5 × 0.3 mm, 5 µm) and washed with 0.1% FA at a flow rate of 5 µL/min for 5 min, prior to loading onto the analytical column. The analytical column was then switched on-line at 600 nL/min over an in house-made 100 µm i.d. × 150 mm fused silica capillary packed with 3.6 µm Aeris C18 resin (Phenomenex; Torrance, CA). After 10 min of sample loading, the flow rate was adjusted to 350 nL/min, and each sample was run on a 120-min linear gradient of 2–40% ACN with 0.1% formic acid to separate the peptides. LC mobile phase solvents consisted of 0.1% formic acid in water (Buffer A) and 0.1% formic acid in acetonitrile (Buffer B, Optima™ LC/MS, Fisher Scientific, Pittsburgh, PA). Data acquisition was performed using the instrument supplied Xcalibur™ (version 3.0) software. The mass spectrometer was operated in the positive ion mode. Each survey scan of *m*/*z* 400–2000 was followed by collision-induced dissociation (CID) MS/MS of the twenty most intense precursor ions. Singly charged ions were excluded from CID selection. Normalized collision energies of 35 eV were employed using helium as the collision gas.

Quantitative analysis of the samples was carried out (n = 6 per group) by liquid chromatography – selected reaction monitoring (LC-SRM) analysis on a QTRAP®5500 triple quadrupole mass spectrometer (ABSciex) couple with a UHPLC Ultimate 3000 (Thermo Fisher) as previously described [28]. Each sample was injected and separated by reversed phase chromatography (Waters, Acquity UPLC BEH C18, 1.7 µm 150 × 1 mm) by running a gradient from 2% to 28% acetonitrile in 0.1% formic acid for 28 min at a flow rate of 150 µL/min. The mass spectrometer was run in positive ion mode with the following settings: source temperature of 210 °C, spray voltage set to 5300 V, curtain gas of 20 psi, and source gas of 35 psi (nitrogen gas). Data were acquired using the instrument-controlled software, Analyst (v1.6.2). QconCAT transition selection, declustering potential, collision energies, and retention times were specifically optimized for each peptide of interest using Skyline's software [29] and settings can be found in previously published data [30].

Data analysis

For global LC-MS/MS, raw files were directly loaded into Proteome Discoverer 2.3 (Thermo Fisher Scientific) and searched against the SwissProt database using an in-house Mascot™ server (Version 2.5, Matrix Science). Mass tolerances were ± 15 ppm for MS peaks, and ±0.6 Da for MS/MS fragment ions. Trypsin specific cleavage was used in searches for cellular and sECM fractions, while CNBr/Trypsin specificity was used for iECM fractions, both allowing for 1 missed cleavage. For all samples, methionine oxidation, proline hydroxylation, protein N-terminal acetylation, and peptide N-terminal pyroglutamic acid formation were allowed as variable modifications while carbamidomethylation of cysteine was set as a fixed modification. Methionine to homoserine and homoserine lactone were included as variable modifications for iECM searches. Label Free Quantification was performed using the Minora Feature detector for precursor peak intensity-based abundance. Data was filtered to a threshold of 1% FDR (strict) at the protein, peptide, at PSM levels using the Protein FDR Validator, Peptide Validator, and Percolator nodes, respectively, in Proteome Discoverer 2.3.

For targeted LC-SRM runs, files were directly loaded into the Skyline software package (version 4.2). Peaks were manually validated and light to heavy ratios ($^{12}C_6/^{13}C_6$) for each target peptide were collected as previously described [30].

The Perseus R-based computational platform [31] was used for statistical analysis and figure generation. Data was log transformed and filtered to remove all proteins containing <2 valid values in a sample group. Data imputation was performed separately for each sample using values from a normal distribution with a width of 0.3 and a downshift of 1.8.

In proteomic comparisons we used equal tissue weight to tissue weight comparisons which reveal significant differences in total protein as indicated by total assigned area under the curve (AUC) ion intensity in LC-MS runs and subsequently the uneven distribution of proteins in the volcano plots (Fig. 4). When we normalize to total AUC ion intensity (highly correlated with protein abundance)

the general trend is maintained, indicating that there are significant differences in protein composition between these two groups which do not directly correlate with overall protein abundance (data not shown).

Data Availability: The mass spectrometry proteomics data have been deposited to the ProteomeXchange Consortium via the PRIDE partner repository with the data set identifier PXD015982. Username: reviewer95682@ebi.ac.uk. Password: M0Kv6XxH.

Gene ontology term enrichment

Gene ontology (GO) biological process terms specifically enriched in a sample group were determined using the LAGO software package (Lewis-Sigler Institute, Princeton University) based on GO:TermFinder [32]. For intrinsic aging enrichment, all proteins in a pairwise comparison of young underarm and aged underarm with $p < 0.05$ or $FC > 3$ were selected and submitted separately by sample enrichment. For photoaging enrichment, forearm-enriched and underarm-enriched proteins in both young and aged sample groups were pooled into two anatomical groups and all proteins with $p < 0.05$ or $FC > 3$ between groups were selected for GO enrichment analysis. Proteins higher in underarm tissue from both young and aged comparisons, as well as proteins higher in forearm tissue, were submitted in separate groups. All GO terms with $p \leq 0.05$ after applying a Bonferroni correction were chosen as significant hits.

Results

Matrisome solubility profiling reveals decreased solubility of ECM proteins with intrinsic aging and photoaging

The sequential extraction method used here (Fig. 1) allows for the assessment of protein solubility by calculating the fraction of the protein signal identified in the insoluble ECM. Measured matrisomal proteins were extracted at a wide range of solubility levels, with TNXB and FN1 extracted nearly entirely in the soluble fractions while ELN and COL8A1 are detected almost exclusively in the insoluble ECM fraction (Fig. 2). The inaccessibility of the most insoluble ECM proteins to both detergent and chaotrope extractions highlights the importance of further digestion in providing full ECM coverage. It has been well documented that collagen decreases in solubility with age as a result of its low turnover and the lifetime accumulation of both crosslinks and non-enzymatic glycation [33,34]. We observe a general trend of decreasing solubility of many ECM components, including collagen, with both aging and photoaging (Fig. 2). Proteins with the most significant reductions in solubility during intrinsic aging, measured by comparing solubility in young and aged hip skin, include COL1A1 ($p = 0.036$), COL4A2 ($p = 0.00013$), lysyl oxidase (LOX) ($p = 0.00046$), and biglycan (BGN, $p = 0.0015$). Proteins most significantly shifted toward the insoluble fraction specifically during photoaging, measured by comparing solubility in aged hip and forearm skin, include COL5A3 ($p = 0.0059$), fibrillin-1 (FBN1, $p = 0.01$), extracellular matrix protein 1 (ECM1, $p = 0.033$), and laminin subunit gamma-1 (LAMC1, $p = 0.037$) (Fig. 2). Interestingly, metalloproteinase inhibitor 3 (TIMP3) significantly increases in solubility with photoaging, indicating that it may change in activity or accessibility in response to UV exposure (Fig. 2).

SHG microscopy reveals decreasing length and width of collagen fibers with intrinsic aging and photoaging

We used ECM-focused imaging and our compartment-resolved proteomic techniques to assess proteins that are altered during intrinsic aging of the dermis. Lifetime exposure of human skin to UV radiation causes premature changes toward an aged phenotype, known as photoaging, and has been shown to alter the composition of matrisomal proteins [11]. To accurately assess the effects of intrinsic aging with minimal confounding alterations due to photoaging, skin biopsies were obtained from sun-protected hip and underarm skin and stratified into two distinct age groups: a young group ranging from 22 to 30 years (26.7 ± 1.3 years) and an aged group ranging from 80 to 88 years (84.0 ± 1.7 years) (see Materials and Methods for details). The gross morphology of the acellular dermis was imaged using SHG microscopy. In young sun-protected skin, collagen fibers appear well ordered, continuous and disperse across the dermis (Fig. 3A). In contrast, collagen fibers in aged sun-protected skin appear fragmented and poorly dispersed across the dermis, with visible clusters of collagen signal and gaps in the collagen network (Fig. 3B).

To extract collagen fiber lengths and widths, SHG images were analyzed using CT-FIRE [22]. Both the length and width of imaged collagen fibers was shown to decrease with increasing chronological age (Fig. 3C, D). Photoaging also resulted in a decrease in collagen fiber length, with forearm samples displaying significantly shorter fibers than either hip or underarm samples within the same age group (Fig. 3C). A reduction in fiber width in response to photoaging was also observed but was less drastic than the effect on fiber length, with significantly shorter fibers than hip skin observed in aged forearm but not young (Fig. 3D). No significant difference in fiber length between young forearm and aged hip skin was observed, demonstrating that

photoaging accelerates the degradation of the collagen network within the skin.

Intrinsic aging in low-UV hip samples causes reductions in structural ECM, basement membrane components, and crosslinking enzymes

For proteomic analysis, a significance cutoff of $p < 0.05$ was used and fold changes are calculated using the more abundant sample group as the numerator. Positive and negative fold changes indicate increases and decreases with aging/photoaging, respectively. In proteomic comparisons of sun-protected hip skin in young and aged subjects, we observed that most of the core matrisomal proteins were markedly reduced in aged dermis, including structural ECM components COL6A6 (FC = –3.5), COL5A2 (FC = –4.1), COL5A3 (FC = –2.5), and COL2A1 (FC = –16.6) (Fig. 4A). This finding is recapitulated within the absolute quantification data, with significant decreases in COL1A1 and COL1A2 observed with every step of increasing age or photoexposure, except for young forearm to aged hip (Fig. 5A, B). However, despite the overall reduction in core matrisome component abundance observed with age, elastin (ELN) was detected at approximately 6.5-fold higher intensity in aged subjects than in young (Fig. 4A). Other elastic network ECM components FBN1 (FC = –1.78), fibrillin-2 (FBN2, FC = –5.3), fibulin-1 (FBLN1, FC = –2.8), fibulin-5 (FBLN5, FC = –3.4), and microfibrillar-associated protein-4 (MFAP4, FC = –5.2) were significantly reduced with intrinsic age (Fig. 4A). Proteoglycan ECM components fibromodulin (FMOD, FC = –9.5), decorin (DCN, FC = –2.4), lumican (LUM, FC = –2.7), versican (VCAN, FC = –3.3), podocan (PODN, FC = –3.5), and mimecan (OGN, FC = –3.1) were also significantly depleted in aged hip samples compared to young (Fig. 4A). Many basement membrane components, including COL4A2 (FC = –2.3), laminin subunit alpha-5 (LAMA5, FC = –3.3), laminin subunit beta-1 (LAMB1, FC = –3.1), laminin subunit beta-2 (LAMB2, FC = –3.7), perlecan (HSPG2, FC = –3.6), nidogen-1 (NID1, FC = –4.0), and nidogen-2 (NID2, FC = –3.6), were significantly reduced with age (Fig. 4A). Additional basement membrane proteins laminin subunit alpha-2 (LAMA2, FC = –3.3), laminin subunit alpha-3 (LAMA3, FC = –3.4), laminin subunit alpha-4 (LAMA4, FC = –3.1), laminin subunit beta-3 (LAMB3, FC = –4.5) and laminin subunit gamma-2 (LAMC2, FC = –3.9) were less abundant in aged hip skin but did not reach significance.

In addition to structural components, ECM architecture and remodeling are heavily regulated by numerous crosslinking enzymes, proteases and protease inhibitors. Lysyl oxidase (LOX), an enzyme involved in generating ECM crosslinks and elastin fibrillogenesis, was significantly reduced at 4-fold lower abundance in aged hip skin (Fig. 4A). Additional ECM crosslinking enzymes transglutaminase 3 (TGM3, FC = –4.5) and transglutaminase 5 (TGM5, FC = –5.8) were also significantly depleted in aged hip samples. While matrix metalloproteinase 2 (MMP2, FC = –3.6) and multiple cathepsins (CTSV (FC = –12.7), CTSB (FC = –7.6), CTSC (FC = –7.2), CTSH (FC = –7.5), CTSD (FC = –3.5), CTSZ (FC = –2.6)) were detected at significantly lower abundance in aged hip samples, protease inhibitors TIMP3 (FC = 14.9) and antileukoproteinase (SLPI, FC = 4.0) were observed at significantly higher abundance in aged hip skin (Fig. 4A). Phospholipase A2 Group IIA (PLA2G2A), an enzyme involved in the formation of inflammatory eicosanoids through the production of arachidonic acid [35], was detected at significantly higher abundance in aged hip skin (FC = 8.7) (Fig. 4A). Interestingly, many of the most significantly reduced proteins with age were hair keratins and associated proteins, including keratin 85 (KRT85, FC = –19.9), keratin 83 (KRT83, FC = –237.0), keratin 34 (KRT34, FC = –147.9), keratin 75 (KRT75, FC = –38.1), keratin-associated protein 2-3 (KRTAP2-3, FC = –76.2), and keratin-associated protein 3-1 (KRTAP3-1, FC = –68.0) (Fig. 4A). Because of the high statistical significance of these measurements, they are unlikely to be an artifact of sample contamination (i.e. introduced during sample preparation) and appear to suggest alteration of hair keratin turnover and production during intrinsic aging, as shown in previous studies [36]. Consistent with earlier reports [37], in young sun-protected hip skin, collagen fibers appeared well organized, densely packed, and intact (Fig. 4B, left panel). In contrast, the collagen fibers in aged hip dermis were sparser and exhibited signs of fragmentation and disorder, with aggregated collagen clusters becoming visible (Fig. 4B, right panel).

Intrinsic aging in mid-UV underarm results in decreased ECM structural components and increased inflammatory markers

In order to assess the effects of intrinsic aging on the skin proteome we also performed a comparative analysis between underarm skin in young and aged patients. Differences in anatomical locations likely result in alterations in protein composition and the response to aging. While the overall trend of lower collagen and other structural ECM component abundance with age seen in hip skin was consistent with underarm comparisons, fewer components were significantly reduced in aged samples (Fig. 6A). ECM core structural components observed at significantly reduced abundance in aged underarm samples include, COL11A2 (FC = –7.9), matrilin-4 (MATN4, FC = –7.9) and MFAP4 (FC = –8.21) (Fig. 6A). Other ECM structural components, including COL1A1 (FC = –1.7), COL1A2 (FC = –1.7), COL2A1 (FC = –2.0),

COL7A1 (FC = –2.2), matrilin-2 (MATN2, FC = –1.8), and dermatopontin (DPT, FC = –1.7) were reduced in aged samples but did not reach significance. Although no elastic fiber components were significantly enriched in either underarm age group, FBLN5 (FC = –3.4) and FBN2 (FC = –1.5) were observed at lower intensities in aged samples. However, the increase in elastin content with age seen in the hip skin is maintained in this comparison, with ELN detected at 2.1-fold higher intensities in aged underarm skin. Proteoglycan ECM components DCN (FC = –1.7) and prolargin (PRELP, FC = –2.7) were significantly decreased in aged underarm samples, with other proteoglycans FMOD (FC = –2.6), BGN (FC = –1.9), OGN (FC = –1.7), and LUM (FC = –1.4) displaying depletion in aged samples that did not reach the significance cutoff (Fig. 6A). Clusterin (CLU) is a stress-induced glycoprotein which has been shown to associate with elastic fibers in aged skin and perform a chaperone-like function, protecting against UV-induced aggregation of elastin [38]. Consistently, here CLU was detected at 1.6-fold higher abundance in aged underarm samples than in young (Fig. 6A).

While no basement membrane components were seen at significantly higher abundance in either sample group, all measured basement membrane components were detected at a lower abundance in aged underarm samples than in young. Basement membrane components most decreased in aged samples without reaching significance include NID1 (FC = –1.7), NID2 (FC = –1.7), LAMA2 (FC = –2.2), LAMA4 (FC = –1.8), LAMC2 (FC = –1.7), and HSPG2 (FC = –1.6) (Fig. 6A). Significant alterations in abundance of ECM modifying enzymes with age were also observed in the underarm comparison, with crosslinking enzyme LOX appearing at 3.5-fold lower abundance in aged samples. In contrast, protease inhibitors SLPI (FC = 6.2) and TIMP3 (FC = 10.1), as well as high-temperature requirement A serine peptidase 1 (HTRA1, FC = 10.1), were all significantly enriched in aged underarm skin, consistent with the hip results (Fig. 6A). WNT1 Inducible Signaling Pathway Protein 2 (WISP2), also known as CCN5, is a glycoprotein involved in developmental regulation and keratinocyte differentiation [39] which, when overexpressed, results in reduced collagen abundance and fibroblast proliferation [40]. We observe WISP2 (FC = 7.0) at significantly higher abundance in aged underarm skin (Fig. 6A). Similar trends to those seen in hip skin were observed in SHG imaging of young and aged underarm skin, with aged skin exhibiting lower overall collagen signal and more uneven collagen fibril distribution than young (Fig. 6B).

Gene ontology (GO) biological function term enrichment analysis of protein clusters which either increased or decreased with intrinsic age revealed system-level molecular signatures of intrinsic aging. Among 154 proteins which were significantly decreased with intrinsic age, 43 biological function GO terms were significantly enriched, including small molecule metabolic process (GO:0044281), oxidation-reduction process (GO:0055114), nucleotide metabolic process (GO:0009117), generation of precursor metabolites and energy (GO:0006091), extracellular matrix organization (GO:0030198), and extracellular structure organization (GO:0043062) (Fig. 7). The significant decreases in a wide variety of metabolically-annotated and ECM proteins suggest reductions in metabolic capacity and ECM integrity of the skin with increasing intrinsic age, respectively.

Among 40 proteins significantly increased with intrinsic age, 19 GO biological function terms were found to be significantly enriched, including response to external stimulus (GO:0009605), immune response (GO:0006955), defense response (GO:0006952), proteolysis (GO:0006508), inflammatory response (GO:0006954), and regulation of inflammatory response (GO:0050727) (Fig. 7). Increasing abundance of defense-related GO terms suggests an increase in immune activity with intrinsic age, while increasing inflammatory markers indicate alterations to the inflammatory environment of the skin. Enrichment of proteolytic enzymes provides support for previous studies which have found increased collagen proteolysis to be a core signature of intrinsic aging [41].

Intrinsic aging in high-UV forearm samples causes decreases in structural ECM components and accumulation of elastic fiber-associated proteins

Although a pairwise comparison of young and aged forearm skin provides less clear information regarding the effects of intrinsic photoaging due to the confounding effect of varying UV-induced photoaging, some insights into how high photoexposure alters the trends seen in intrinsic aging can be gained. The two most abundant structural ECM components, COL1A1 (FC = –2.2) and COL1A2 (FC = –2.3) are significantly reduced in aged forearm skin, suggesting that photo-exposure accelerates degradation of the collagen network (Fig. 8A). Interestingly, in SHG imaging of forearm skin samples from aged subjects, an overall decrease in collagen network density is not observed at this level of analysis, with aged samples exhibiting more visible collagen intensity but less dispersion and more network aggregation (Fig. 8B). While the intrinsic aging process results in an overall degeneration of the extracellular elastic fiber network [5], large amounts of photo-exposure can result in the accumulation of non-functional elastic-fiber material, generating a condition known as solar elastosis [42,43]. In contrast to our observations in the hip skin pairwise comparison, both global (Fig. 8A) and

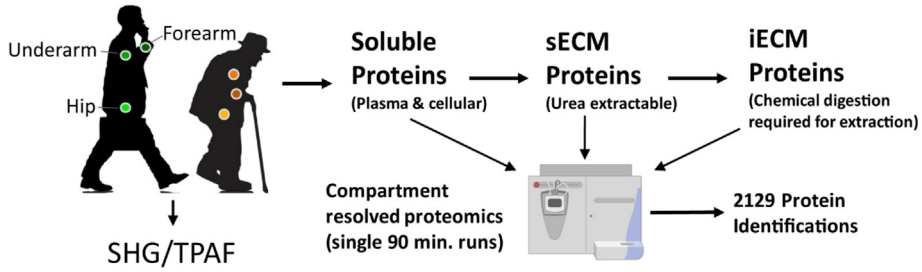

Fig. 1. Experimental overview. Skin punch biopsies were collected from the hip, underarm, and forearm of young and aged subjects. Skin samples were subjected to compartment-resolved extraction, generating cellular (soluble), soluble ECM (sECM), and insoluble ECM (iECM) fractions. Each fraction was analyzed via mass spectrometry and 2129 proteins were identified across all samples at 1% FDR. Skin biopsies were additionally subjected to SHG and TPAF imaging to visualize collagen and elastin within the dermis.

quantitative (Fig. 5C, D) proteomics show that some elastic network-related proteins including FBLN1 (FC = 4.5) and the elastic fiber associated glycoprotein vitronectin (VTN, FC = 6.9) are significantly enriched in aged forearm samples. Additionally, FBLN2 (FC = 2.1), FBLN7 (FC = 2.9), FBN2 (FC = 1.8), and ELN (FC = 2.0) were detected at higher intensities in aged forearm skin but did not reach significance. Similar trends to those seen in hip and underarm comparisons were observed for the proteoglycans FMOD (FC = –4.1) and PODN (FC = –3.3), as well as the crosslinking enzyme LOX (FC = –3.7), with all proteins significantly reduced in aged forearm samples (Fig. 8A). TIMP3 (FC = 11.7), SLPI (FC = 5.3), WISP2 (FC = 4.2) and CLU (FC = 10.1) also follow a similar pattern to that seen in earlier comparisons, all showing significant enrichment in aged forearm skin (Fig. 8A). High-temperature requirement A serine peptidase 3 (HTRA3, FC = 12.4) was identified at significantly higher intensity in aged forearm skin (Fig. 8A), while ECM crosslinking enzymes transglutaminase 1 (TGM1, FC = 3.3), TGM3 (FC = 1.9), and TGM5 (FC = 1.4) were present at higher levels in aged forearm skin but did not reach significance.

Photoexposure in young samples causes reductions in structural ECM and ECM protease inhibitors

To assess the proteomic effects of photoaging with fewer confounding effects of chronological aging, we performed a pairwise comparison of sun-protected and sun-exposed skin in young subjects. Because hip and forearm skin likely vary in protein composition as a result of anatomical location, as supported by previous fibroblast transcriptomics [44], underarm skin was chosen as the sun-protected tissue for photoaging comparisons against sun-exposed forearm. Significant alterations in matrisome composition were observed between young underarm and forearm, indicating that by an individual's mid-20's forearm skin has received sufficient photoexposure to induce molecular-level changes even before clinical signs of photoaging are present. We observed that the majority of observed proteins were

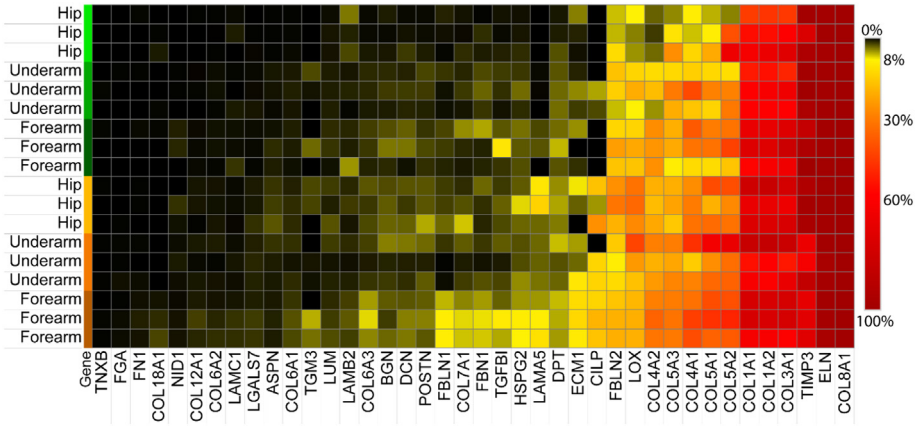

Fig. 2. Solubility profiling of ECM components. Solubility of each protein is calculated as the percentage of total AUC ion intensity across all fractions which resulted from the iECM fraction. Rows represent hip, underarm, and forearm samples from young (green) and aged (orange) subjects.

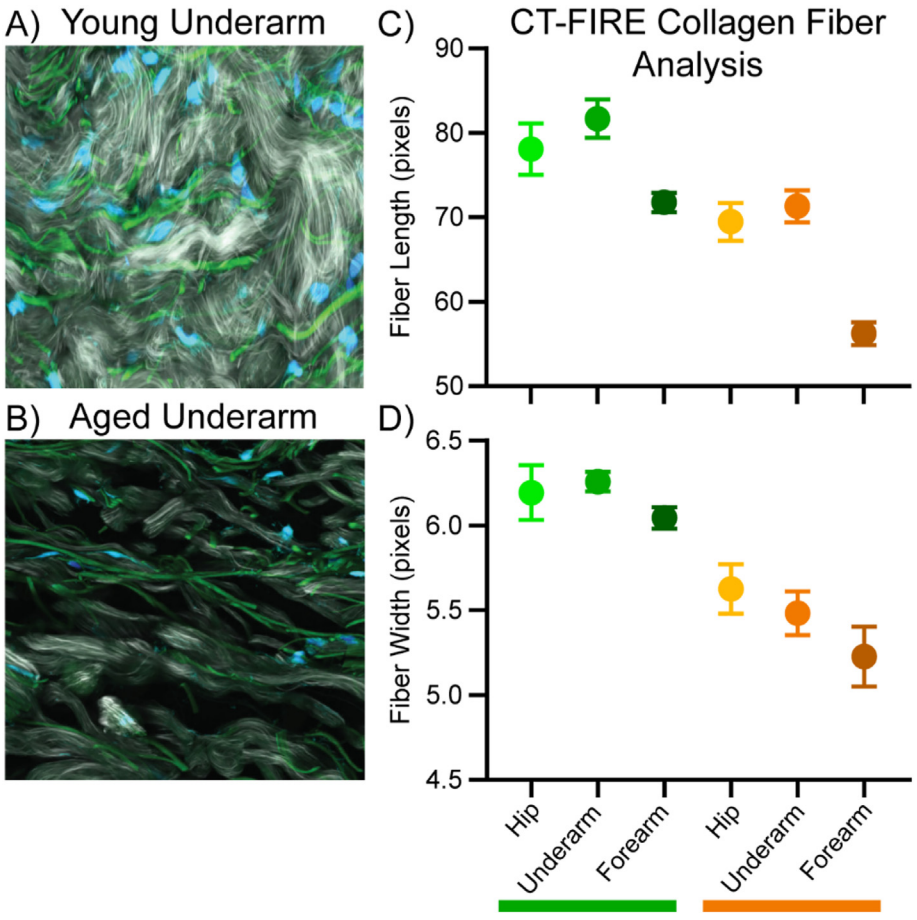

Fig. 3. SHG/TFAP images for young (A) and aged underarm (B) showing collagen (white), elastin (green), and DAPI stain (blue). Collagen fiber length (C) and width (D) for young (green bar) and aged (orange bar) samples derived from SHG imaging using CT-FIRE image analysis. Error bars display 95% confidence interval for the sample group.

detected at lower levels in forearm skin, suggesting that photo-exposure results in degradation or reduced synthesis of protein networks within young skin (Fig. 9A). No core structural ECM proteins were found to be significantly enriched in either sample (Fig. 9A). However, additional structural ECM proteins including COL6A5 (FC = −12.2), COL7A1 (FC = −3.4), COL17A1 (FC = −3.7), and MATN2 (FC = −1.6) were reduced with age but did not reach significance, indicating an overall reduction in structural ECM abundance with increasing photoaging in young skin. Elastic fiber components FBN2 (FC = −3.5) and MFAP4 (FC = −5.6) were identified at significantly lower levels in forearm skin, while other elastic fiber components (FBN1 (FC = −1.8), FBLN5 (FC = −2.8)) were observed at lower intensities in forearm skin but below the significance cutoff (Fig. 9A). Elastin, in contrast to previous intrinsic aging comparisons, is present at similar levels in underarm and forearm skin, suggesting that it is not significantly affected by the difference in photo-exposure between these two locations in young skin. Proteoglycan ECM components were generally identified at lower abundance with increased photoaging, with OGN significantly reduced (FC = −3.1) and BGN (FC = −2.8), asporin (ASPN, FC = −2.8), DCN (FC = −1.7), and LUM (FC = −1.9) showing lower intensity with photoaging without significant depletion (Fig. 9A).

Although no significant alterations in core basement membrane components were detected during photoaging of young skin, all measured basement membrane components were present at lower intensities in sun-exposed forearm skin (Fig. 9A). LAMA3 (FC = −1.8), LAMB3 (FC = −2.9), LAMC2 (FC = −2.4), NID1 (FC = −2.2), and ECM1 (FC = −3.2) decreased most drastically with photoaging but did not reach significance. Together, LAMA3, LAMB3, and LAMC2 make up laminin 332, a structural basement membrane component involved in cell adhesion [45], wound healing [46], and keratinocyte proliferation [47]. ECM crosslinking enzymes TGM1 (FC = −3.0) and TGM3 (FC = −2.7) were measured at lower intensities in forearm

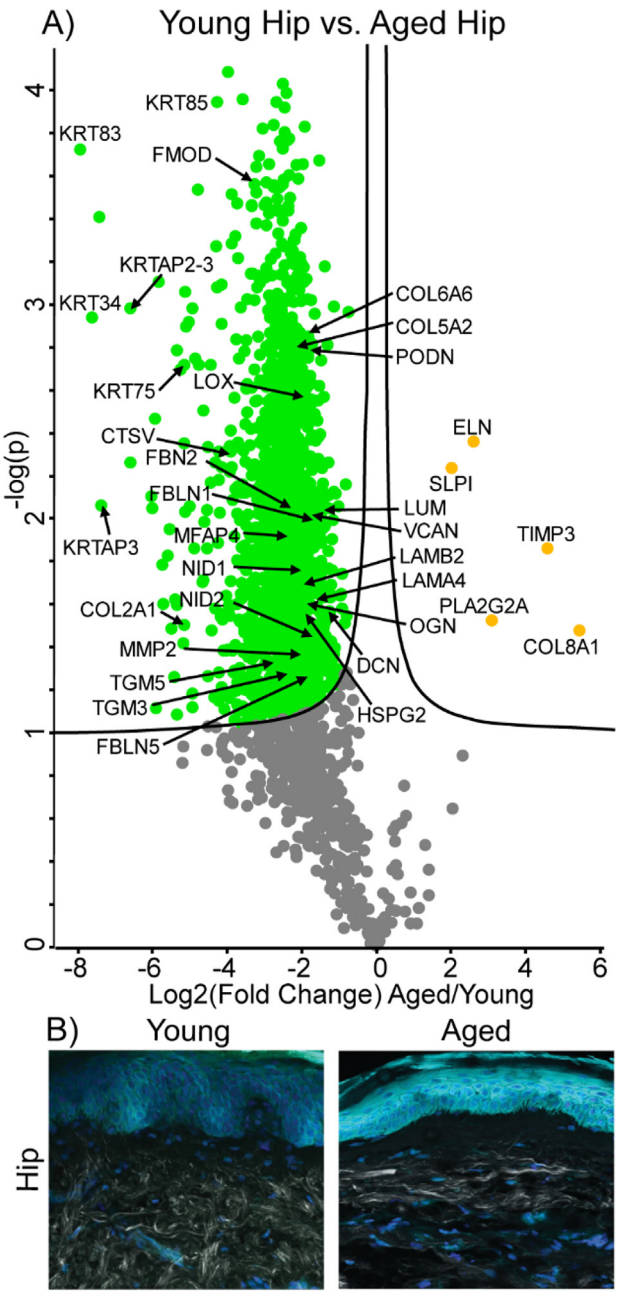

Fig. 4. Differentially expressed proteins and ECM network alterations during intrinsic aging in human hip skin. Volcano plot visualization of significantly enriched proteins between young and aged hip skin (A). Proteins above significance cutoff colored green (young) or orange (aged). SHG/TFAP imaging of young and aged hip skin (B) showing collagen fibrils (white), elastin (green), and nuclei (blue).

skin without reaching significance, while no change in LOX abundance was apparent between the two sample groups. Extracellular serine protease HTRA1 is enriched at 8.8-fold higher abundance in forearm samples but does not reach significance, while serine protease inhibitors SERPING1 (FC = −2.8), SERPINA6 (FC = −2.5), SERPINC1 (FC = −2.3), SERPINF2 (FC = −3.0), and SERPINB2 (FC = −93.0) were all significantly reduced in forearm skin (Fig. 9A). This suggests that SERPIN class serine protease inhibitors are depleted by photoexposure and that extracellular proteolytic activity is less inhibited in a more photo-exposed tissue environment. As seen in earlier intrinsic aging comparisons, WISP2 (FC = 3.2) is significantly enriched in more photoaged forearm skin.

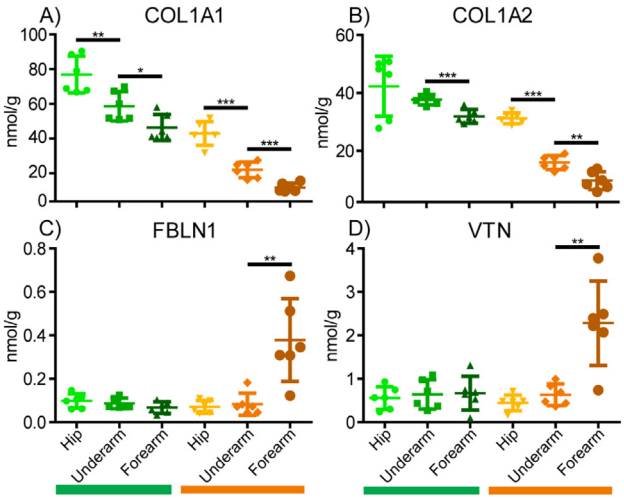

Fig. 5. Absolute quantitation of key ECM proteins in young (green) and aged (orange) samples. Quantification was performed using SIL QconCAT peptide standards. Error bars represent standard deviation.

Photoexposure in aged samples causes increases in basement membrane and elastic fiber components

The effects of photoaging were also assessed using a pairwise comparison of aged underarm and forearm skin. Because the forearm of an aged subject has experienced drastically more lifetime UV exposure than that of a young subject, while the underarm remained largely UV-protected, it is likely that the proteome alterations due to photoaging will be more drastic in aged skin. In contrast to other comparisons, structural ECM components were not significantly enriched in either sample group, suggesting that large amounts of photoexposure may impair protein clearing, countering the overall reduction in structural ECM seen in intrinsic aging comparisons. Elastic fiber network component FBLN1 (FC = 3.6) was detected at significantly higher intensity in forearm skin, alongside FBLN7 (FC = 2.0), which was identified at higher intensity but did not reach significant enrichment (Fig. 9B). The enrichment of FBLN1 specifically in aged, sun-exposed forearm skin was confirmed by the absolute quantification data, in which FBLN1 was detected at significantly higher intensity in the aged forearm than in any other sample (Fig. 5C). Additionally, VTN is observed at significantly higher intensities in aged forearm samples in both global (FC = 3.5, Fig. 9B) and quantitative analyses (Fig. 5D). These proteins were chosen for quantification as surrogate measures for elastic fiber abundance due to difficulties in solubilizing and analyzing ELN. The accumulation of elastic fiber-associated proteins within photoaged forearm skin indicates the beginning of solar elastosis, in which aberrant elastic fibers aggregate within the dermis. Proteoglycan ECM components OGN (FC = –3.9), ASPN (FC = –6.1), PODN (FC = –3.3), LUM (FC = –2.3), and DCN (FC = –1.8) were all significantly decreased with photoaging, illustrating a decrease in total proteoglycan abundance with UV exposure (Fig. 9B).

In contrast to the trend seen in the comparison of young forearm and underarm skin, all measured basement membrane proteins are detected at higher abundance with photoaging in aged skin. COL4A2 (FC = 2.5) is significantly enriched in forearm skin, while LAMA2 (FC = 1.8), LAMB1 (FC = 1.7), and LAMC1 (FC = 1.7) represent the basement membrane components with the highest forearm enrichment without reaching significance (Fig. 9B). The observed increase in basement membrane components with high UV exposure may be due to the thickening of the basement membrane in response to aging and UV-induced damage, as shown in previous studies [48,49]. Serine protease HTRA1 (FC = 3.0) was significantly enriched in forearm skin, representing the only detected ECM regulator which is significantly enriched in either sample group (Fig. 9B).

GO-term enrichment reveals loss of metabolic proteins and increased stress/immune response with photoaging

GO term enrichment analysis was used to assess molecular alterations during photoaging by separately pooling all underarm- and forearm-enriched proteins in both young and aged pairwise photoaging comparisons. Within 976 proteins that decreased with photoaging, 490 GO biological function terms were significantly enriched, including organic substance metabolic process (GO:0071704), primary metabolic process (GO:0044238), organonitrogen compound metabolic process (GO:1901564), localization (GO:0051179), transport (GO:0006810),

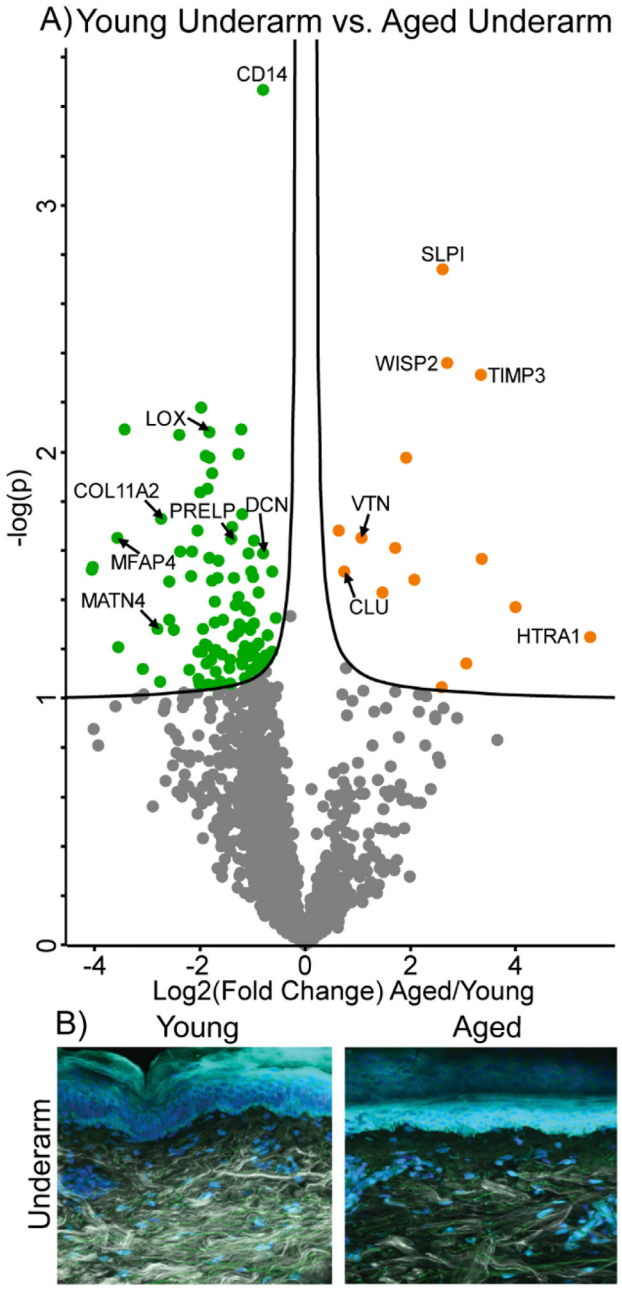

Fig. 6. Differentially expressed proteins and ECM network alterations during intrinsic aging in human underarm skin. Volcano plot visualization of significantly enriched proteins between young and aged underarm skin (A). Proteins above significance cutoff colored green (young) or orange (aged). SHG/TFAP imaging of young and aged underarm skin (B) showing collagen fibrils (white), elastin (green), and nuclei (blue).

and protein metabolic process (GO:0019538) (Fig. 9C). Decreases in these terms suggest an overall deficit in metabolic and protein trafficking components in highly photoaged tissue which is supported by reductions in metabolic capacity in cultured fibroblasts from aged donors [50]. From 123 proteins detected at significantly higher abundance with increasing photoage, 52 GO biological function terms were significantly enriched, including cell differentiation, response to stress, immune system process, cell death, immune response, and epithelium development (Fig. 9C). Increases in proteins related to immune and stress-related processes suggest that a high degree of photoaging induces tissue damage-related responses within the skin.

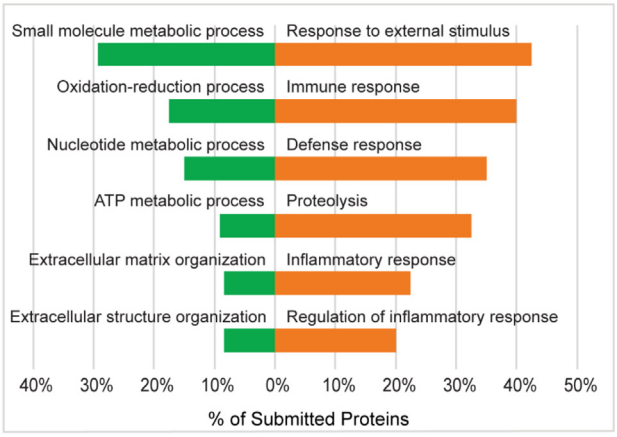

Fig. 7. Selected gene ontology (GO) biological process terms enriched in young underarm (green) and aged underarm (orange). All proteins with $p < 0.05$ or $FC > 3$ between sample groups were selected for GO enrichment analysis. Displayed terms were selected due to high enrichment significance and relevance.

Discussion

Alterations in ECM solubility

Through global and quantitative proteomic analysis, we have identified several changes to matrisome composition that occur during both intrinsic and extrinsic aging, as well as molecular signatures unique to each aging process. A summary of matrix changes during intrinsic and extrinsic aging can be found in Fig. 10. We assess solubility of matrisomal proteins as the percent of total area under the curve (AUC) signal for each protein detected in the iECM fraction. The inaccessibility of some ECM proteins to both detergent and chaotrope extractions highlights the importance of performing further digestion to fully characterize matrix composition. Due to the lifetime accumulation of crosslinks and glycation, collagen has been shown to decrease in solubility with increasing age [51]. We observe significant decreases in solubility of not only a variety of collagens with both intrinsic aging and photoaging, but also other ECM proteins, including LOX with intrinsic aging and basement membrane components with photoaging. The differential effects of intrinsic and extrinsic aging on the solubility of some ECM proteins provide additional insight into the distinct molecular signatures of these processes.

Alterations in structural ECM and elastic fibers

With increasing age and photoexposure, we observe a clear decrease in the abundance of many core structural ECM components, indicating a decrease in ECM structural integrity. The loss of ECM structural components in aging skin is mirrored in studies of aging fibroblasts, where the secretion of multiple collagens is reduced in senescent cells when compared to control [52]. Both global and quantitative data show stepwise decreases in collagen I abundance with each level of age and photoexposure, providing proteomic evidence which supports the finding that collagen is increasingly fragmented during both intrinsic and extrinsic aging and subsequently inhibits procollagen production [8]. These findings are further supported by SHG/TPAF imaging in which thinner, shorter, and more disorganized collagen fibers are observed in both intrinsically aged and photoaged skin. The presence of thin, fragmented, sparsely organized collagen fibers in aged dermis is confirmed by other recent microscopy studies [53]. Collagen abundance and fiber length in young, sun-exposed forearm skin are most like those in aged, sun-protected hip skin, suggesting that extrinsic aging shares some molecular signatures with intrinsic aging and photoexposure may accelerate the progression of an aged skin phenotype. However, photoaging also induces unique molecular features including an overall accumulation of protein, as shown in the pairwise comparisons of young and aged skin (Figs. 3, 5, 7). Basement membrane components also undergo overall decreases in abundance with intrinsic age, coinciding with the flattening and weakening of the dermal-epidermal junction observed in previous studies [6].

Elastic fibers, composed of an elastin core and a microfibrillar scaffold, are a core component of the dermal ECM and are largely responsible for skin elasticity [54]. Previous studies have reported differential effects on elastic fiber content during intrinsic aging and photoaging, with intrinsic aging resulting in overall degradation of the elastic fiber network due to decreased synthesis and assembly of elastin fibers [5]. In contrast, photoaging is characterized by an

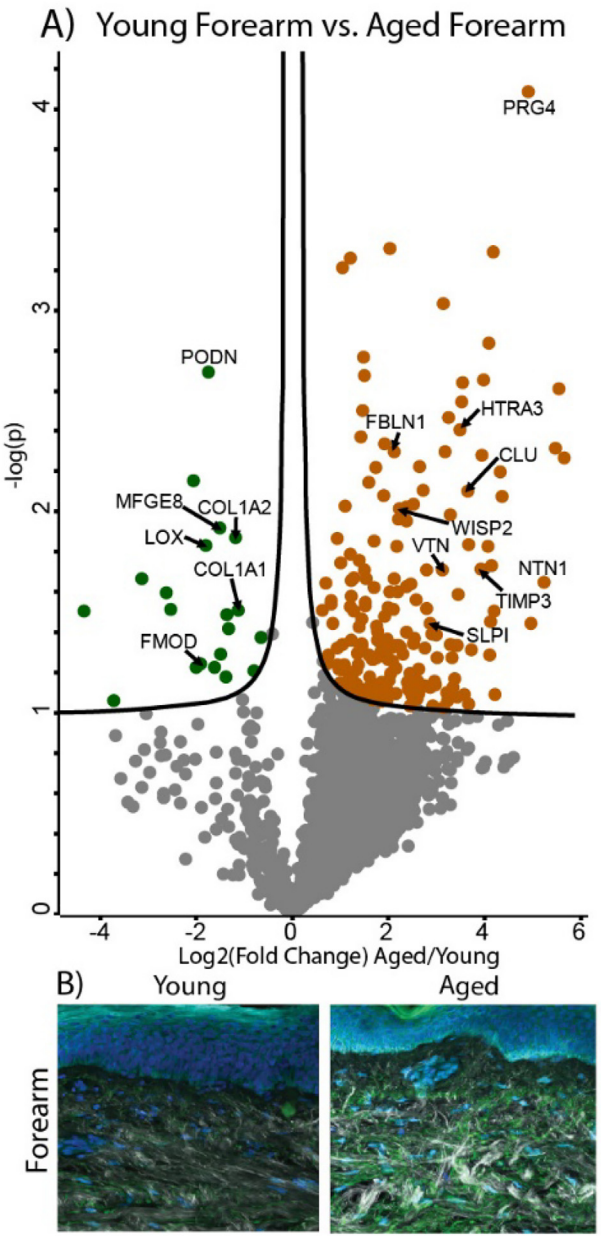

Fig. 8. Differentially expressed proteins and ECM network alterations during intrinsic aging in human forearm skin. Volcano plot visualization of significantly enriched proteins between young and aged forearm skin (A). Proteins above significance cutoff colored green (young) or orange (aged). SHG/TFAP imaging of young and aged forearm skin (B) showing collagen fibrils (white), elastin (green), and nuclei (blue).

accumulation of aberrant elastotic material within the dermis, termed solar elastosis [5]. In our data, we observe an overall decrease in most elastic fiber associated components, including MFAP4, FBLN1, FBLN5, and FBN2, during intrinsic aging in sun-protected hip skin (Fig. 4). However, we also see an enrichment of elastin in aged hip skin compared to young, contrasting with previous findings. This enrichment may be due to the high degree of LOX crosslinking and insolubility of the mature elastin protein, in addition to the lack of unmodified lysine residues within its sequence, making mature elastin insusceptible to cleavage by either trypsin or chemical digestion [55]. Lysyl oxidase is involved in the cross-linking of both collagen and elastin for proper fiber assembly [56,57]. We observe decreases in LOX abundance in all anatomical pairwise comparisons, suggesting decreased LOX activity, and likely subsequent elastin assembly, with increasing age. FBLN5 has also been shown to be essential for elastogenesis in vivo [58], indicating that age-associated decreases in this key protein could impair elastin assembly.

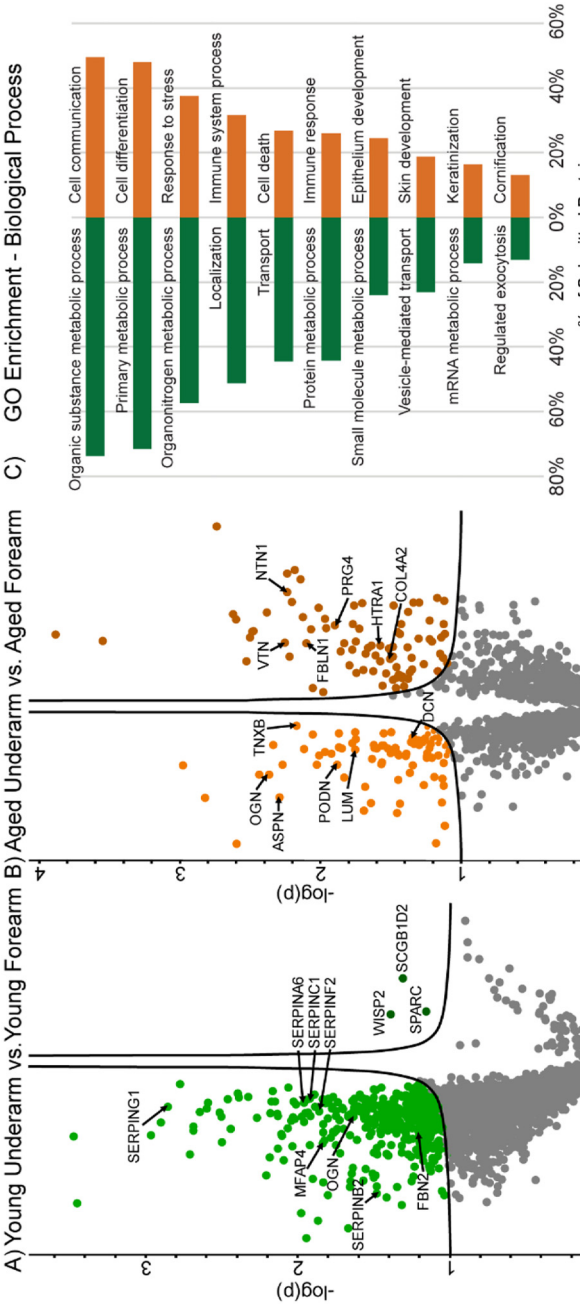

Fig. 9. Differentially expressed proteins and network alterations during photoaging in human arm skin. Volcano plot visualization of significantly enriched proteins between young underarm and forearm skin (A) and aged underarm and forearm skin (B). Significantly enriched proteins are colored light green (underarm) or dark green (forearm) (A) and light orange (underarm) or dark orange (forearm) (B). Selected gene ontology (GO) biological process terms enriched in underarm (green) and forearm (orange) (C). Forearm-enriched and underarm-enriched proteins in both young and aged sample groups were pooled into two anatomical groups and all proteins with $p < 0.05$ or $FC > 3$ between groups were selected for GO enrichment analysis. Displayed terms were selected due to high enrichment significance and relevance.

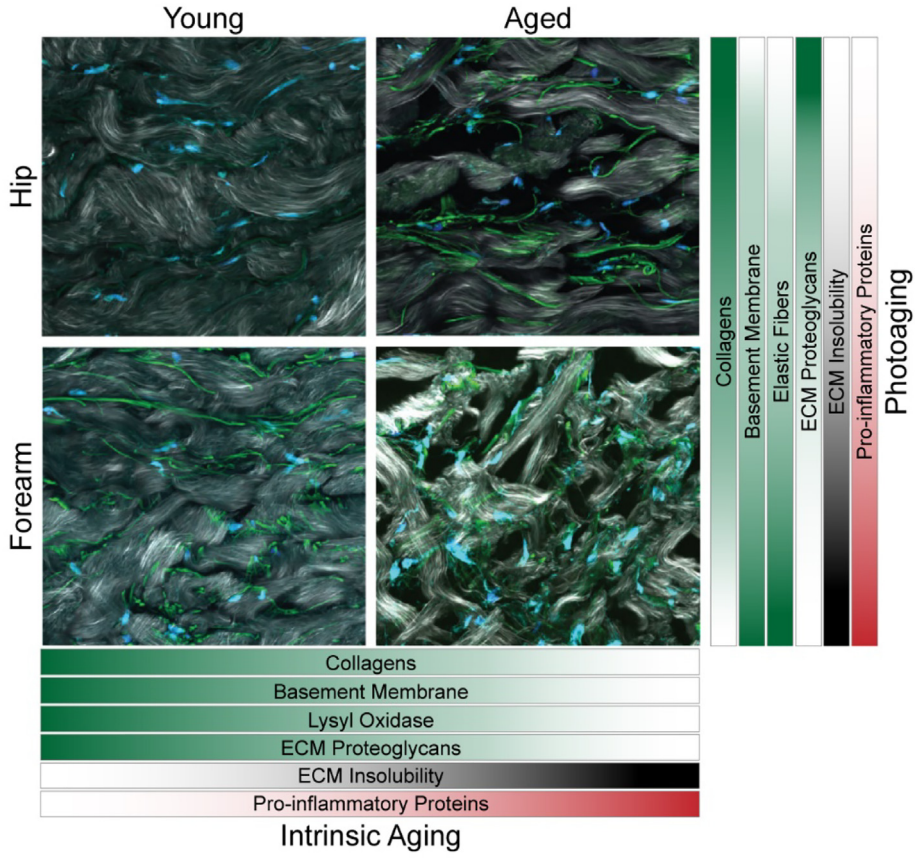

Fig. 10. Summary of matrix alterations during intrinsic aging and photoaging. Representative SHG images of hip and forearm skin from young and aged subjects showing collagen fibrils (white), elastin (green), and nuclei (blue). Bars display change in abundance or solubility of ECM components during intrinsic aging and photoaging (darker, higher magnitude; lighter, lower magnitude).

In highly photoexposed skin, elastin-containing material and associated proteins have been shown to accumulate within the dermis as a result of UV-induced alternative elastin splicing [59] and increased tropoelastin mRNA expression in response to both UV radiation [42] and heat [43]. While we do not see significant enrichment of elastin with photoaging, likely due to the high inaccessibility of the protein in all samples, we observe increased abundance of in elastic-fiber associated glycoproteins VTN and FBLN1 in forearm skin of aged subjects when compared to underarm. The increasing abundance of some elastic fiber components with photoaging contrasts with the trends seen for these same proteins during chronological aging, possibly suggesting that solar elastosis is occurring in aged forearm samples at a rate that outpaces the degradation of elastic fibers due to intrinsic aging. Clusterin, a stress-induced glycoprotein shown to help prevent UV-induced aggregation of elastin [38], is also identified at higher abundance with photoaging, suggesting that the interaction between these two proteins likely plays a role in the regulation of UV-induced elastosis.

Alterations in ECM proteoglycans

Proteoglycans are defined as containing a core protein with at least one attached GAG alongside other O- and N-linked oligosaccharides. Although proteoglycans serve many critical roles within the ECM, from structural components to signaling regulators, a primary function for many ECM proteoglycans is the regulation of TGF-β signaling and collagen fibrillogenesis. For example, independent knockouts of LUM [60], FMOD [60], DCN [61], BGN [62], and OGN [63] in mice have all been shown to generate defects in collagen fibril diameter and contour, suggesting they play a key part in regulating collagen assembly and architecture. DCN has also been demonstrated to inhibit MMP-mediated cleavage of collagen, further enhancing the resilience of the collagen network [64]. We observe significant decreases in all these proteoglycans with both intrinsic and extrinsic aging,

suggesting that both processes result in deficits in regulation of collagen fibrillogenesis and maintenance.

Alterations in ECM modifying proteins

Over the lifespan, ECM components are constantly modified and remodeled through crosslinking, glycation, and proteolytic degradation performed by a variety of ECM-associated enzymes. Crosslinking of structural ECM proteins is essential to the structural stability and physicochemical properties of the matrix and increases in frequency with increasing age [34]. LOX functions as the primary crosslinking enzyme for both collagen [65] and elastin [57], aiding in the assembly and deposition of these proteins within the ECM. We observe reductions in LOX with intrinsic aging in all pairwise age comparisons, as shown in previous studies by activity assay [66] and gene expression analysis [67]. The loss of LOX during aging likely contributes to deficits in both collagen and elastic fiber assembly. Other enzymes which crosslink ECM components include transglutaminases, which are responsible for the formation of the cornified envelope (CE) through crosslinking of filaggrin, loricrin, and a variety of small proline-rich proteins [68]. While we identify TGM1, TGM2, TGM3, and TGM5 consistently across all samples, significant enrichments of any TGM protein are observed only in comparisons of young hip and aged hip, where we observe reductions in TGM3 and TGM5 with intrinsic aging. TGM3 has been shown to provide some protection from photodamage by strengthening the UV-filtering capabilities of the cornified envelope [69], suggesting that skin may become more susceptible to UV damage with increasing age.

In addition to crosslinking enzymes, ECM remodeling is heavily regulated by a series of proteases and proteolytic regulators. The two primary classes of proteases that function within the extracellular matrix are matrix metalloproteases, which are primarily responsible for structural degradation of the ECM, and serine proteases, which mainly function to initiate activation cascades [70]. We detect MMP2 at reduced abundance in aged hip skin compared to young, but do not see significant changes in MMP abundance in any other comparisons. However, metalloprotease inhibitor TIMP3 is consistently observed at higher intensity in aged skin in all pairwise comparisons between anatomical locations, suggesting that it increases in abundance with intrinsic age. While the abundance of other TIMP proteins has been previously shown to be inversely correlated with tissue age [71], TIMP3 is uniquely expressed solely in the extracellular matrix and likely functions as a marker of terminal differentiation within the cell [72], increasing in abundance with increasing age [73].

Cathepsin proteases have been previously implicated in the turnover and remodeling of the ECM through the proteolytic processing of a variety of ECM components [74–76] and shown to be downregulated during intrinsic aging [77] and photoaging [78–80]. We observe significant reductions in a wide variety of cathepsins during intrinsic aging, likely resulting in reduced ECM turnover with age. Increasing cathepsin D abundance in photoaged skin through topical application was previously shown to restore water content and TGase-1 expression in photoaged tissue [81], suggesting that the loss of these proteins may play a critical role in skin barrier degradation.

Serine proteases high temperature requirement A1 and A3 (HTRA1 and HTRA3) were observed to increase specifically with photoaging, appearing significantly enriched only in highly photoaged forearm skin. HTRA proteases have been shown to cleave a number of ECM substrates, including fibronectin, clusterin, and vitronectin [82]. HTRA proteins have also been shown to antagonize TGF-β signaling [83,84], promoting a pro-inflammatory environment by suppressing TGF-β-mediated anti-inflammatory immune regulation [85]. Increased abundance of HTRA proteases in response to photoaging, in addition to enrichment of inflammatory proteins observed in intrinsically aged tissue, supports the hypothesis that a pro-inflammatory state is associated with accelerated dermal alteration.

Method strengths and future improvements

By using compartmental extraction coupled with chemical digestion, we are able to detect all key skin proteins not consistently identified across previous skin proteomics studies [19], as well as a wide variety of other ECM components. Our data provides coverage of 229 of the 1111 proteins annotated within the matrisome project DB [18] and includes 115 of 275 core matrisome-annotated proteins. While our method covers a larger fraction of matrisomal protein than previous methods, we are unable to identify many secreted factors and signaling molecules, including cytokines, growth factors, and interleukins which are present at low abundance and more loosely associated with the ECM. Elastin is highly crosslinked and lack lysine and arginine residues, making it difficult to digest and analyze using proteomics. It is possible that deficits in ELN assembly observed with chronological age allow elastin to be more readily digested and identified, making its apparent signal higher in aged samples than in young. The true amount of elastin present in each sample could be determined in future studies by amino acid and crosslinking analysis (desmosine/isodesmosine as surrogate measures) of the remaining pellet after chemical digestion or with the development of an ELN optimized proteomic method.

Conclusions

Overall, both intrinsic aging and photoaging can be characterized by significant decreases in structural ECM integrity, shown by significant reductions in both the abundance of most collagens and the length and width of collagen fibers. Proteoglycans which perform ECM-supporting functions, such as regulation of collagen fibrillogenesis, are also decreased by both types of aging, likely driving the degradation of the structural ECM. Intrinsic aging results in a distinct molecular signature from that generated by photoaging, producing reductions in elastic fiber and crosslinking enzyme abundance which also likely contribute to a loss of ECM structural integrity and elasticity. Photoaging, on the other hand, can generally be defined by increases in elastic fiber-associated proteins, indicating the progression of elastosis, and pro-inflammatory proteases such as the HTRA family. Both intrinsic aging and photoaging cause a loss of metabolic enzymes and an increase in the abundance of immune- and inflammation-related proteins. Anti-inflammatory interventions may be a useful target for future anti-aging skin therapies.

Funding

This work was supported by the National Institutes of Health [grant numbers AG054835, AG051849, R33CA183685, S10OD021641]; and the Milstein Medical Asian American Partnership Foundation.

Declaration of competing interest

The authors declare that they have no known competing financial interests or personal relationships that could have appeared to influence the work reported in this paper.

Acknowledgements

Workflow figure (Fig. 1) was created with Biorender.com.

Appendix A. Supplementary data

Supplementary data to this article can be found online at https://doi.org/10.1016/j.mbplus.2020.100041.

Received 2 January 2020;
Received in revised form 2 April 2020;
Accepted 5 June 2020
Available online 17 June 2020

Keywords:
Skin;
Aging;
Photoaging;
Extracellular matrix;
Proteomics;
Collagen

Abbreviations used:
ECM, extracellular matrix; SHG, single harmonic generation; TPAF, two-photon autofluorescence; UV, ultraviolet; CE, cornified envelope; sECM, soluble ECM; iECM, insoluble ECM; QconCATs, quantitative concatemers; CNBr, cyanogen bromide; AUC, area under the curve; GO, gene ontology.

References

[1] F.M. Watt, H. Fujiwara, Cell-extracellular matrix interactions in normal and diseased skin, Cold Spring Harb. Perspect. Biol. 3 (2011) 1–14.
[2] M. Wlaschek, I. Tantcheva-Poor, L. Naderi, W. Ma, L.A. Schneider, Z. Razi-Wolf, J. Schuller, K. Scharffetter-Kochanek, Solar UV irradiation and dermal photoaging, J. Photochem. Photobiol. B Biol. 63 (2001) 41–51www.elsevier.com.
[3] B. Dreno, E. Araviiskaia, E. Berardesca, G. Gontijo, M. Sanchez Viera, L.F. Xiang, R. Martin, T. Bieber, Microbiome in healthy skin, update for dermatologists, J. Eur. Acad. Dermatology Venereol. 30 (2016) 2038–2047, https://doi.org/10.1111/jdv.13965.
[4] G.J. Fisher, S. Kang, J. Varani, Z. Bata-csorgo, Y. Wan, S. Datta, J.J. Voorhees, Mechanisms of photoaging and chronological skin aging, Arch Dermatology. 138 (2002) 1462–1470.
[5] J. Uitto, The role of elastin and collagen in cutaneous aging: intrinsic aging versus photoexposure, J. Drugs Dermatology. 7 (2008) s12–s16http://www.ncbi.nlm.nih.gov/pubmed/18404866.
[6] R.M. Lavker, P. Zheng, G. Dong, Aged skin: a study by light, transmission electron, and scanning electron microscopy, J. Invest. Dermatol. 88 (1987) s44–s51, https://doi.org/10.1038/jid.1987.9.
[7] S. Luebberding, N. Krueger, M. Kerscher, Age-related changes in skin barrier function – quantitative evaluation of 150 female subjects, Int. J. Cosmet. Sci. 35 (2013) 183–190, https://doi.org/10.1111/ics.12024.
[8] S.E.G. Fligiel, J. Varani, S.C. Datta, S. Kang, G.J. Fisher, J.J. Voorhees, Collagen degradation in aged/photodamaged skin in vivo and after exposure to matrix metalloproteinase-1 in vitro, J. Invest. Dermatol. 120 (2003) 842–848, https://doi.org/10.1046/j.1523-1747.2003.12148.x.
[9] J. Varani, M.K. Dame, L. Rittie, S.E.G. Fligiel, S. Kang, G.J. Fisher, J.J. Voorhees, Decreased collagen production in chronologically aged skin: roles of age-dependent alteration

in fibroblast function and, Am. J. Pathol. 168 (2006) 1861–1868, https://doi.org/10.2353/ajpath.2006.051302.
[10] K. Scharffetter-Kochanek, P. Brenneisen, J. Wenk, G. Herrmann, W. Ma, L. Kuhr, C. Meewes, M. Wlaschek, Photoaging of the skin from phenotype to mechanisms, Exp. Gerontol. 35 (2000) 307–316, https://doi.org/10.1016/S0531-5565(00)00098-X.
[11] L. Rittié, G.J. Fisher, Natural and sun-induced aging of human skin, Cold Spring Harb. Perspect. Med. 5 (2015) 1–14, https://doi.org/10.1101/cshperspect.a015370.
[12] R.M. Lavker, Structural alterations in exposed and unexposed aged skin, J. Invest. Dermatol. 73 (1979) 59–66, https://doi.org/10.1111/1523-1747.ep12532763.
[13] J.H. Chung, K. Yano, M.K. Lee, C.S. Youn, J.Y. Seo, K.H. Kim, K.H. Cho, H.C. Eun, M. Detmar, Differential effects of photoaging vs intrinsic aging on the vascularization of human skin, Arch Dermatology. 138 (2002) 1437–1442.
[14] A.M. Kligman, Perspectives and problems in cutaneous gerontology, J. Invest. Dermatol. 73 (1979) 39–46, https://doi.org/10.1111/1523-1747.ep12532758.
[15] T. Quan, G.J. Fisher, Role of age-associated alterations of the dermal extracellular matrix microenvironment in human skin aging: a mini-review, Gerontology. 61 (2015) 427–434.
[16] M. Watson, D.M. Holman, M. Maguire-Eisen, Ultraviolet radiation exposure and its impact on skin cancer risk, Semin. Oncol. Nurs. 32 (2016) 241–254, https://doi.org/10.1016/j.physbeh.2017.03.040.
[17] C.C. Sprenger, S.R. Plymate, M.J. Reed, Aging-related alterations in the extracellular matrix modulate the microenvironment and influence tumor progression, Int. J. Cancer 127 (2010) 2739–2748, https://doi.org/10.1002/ijc.25615.
[18] A. Naba, K.R. Clauser, S. Hoersch, H. Liu, S.A. Carr, R.O. Hynes, The matrisome: in silico definition and in vivo characterization by proteomics of normal and tumor extracellular matrices, Mol. Cell. Proteomics 11 (2012) 1–18, https://doi.org/10.1074/mcp.M111.014647.
[19] S.A. Hibbert, M. Ozols, C.E.M. Griffiths, R.E.B. Watson, M. Bell, M.J. Sherratt, Defining tissue proteomes by systematic literature review, Sci. Rep. 8 (2018) 1–10, https://doi.org/10.1038/s41598-017-18699-8.
[20] C. Griffiths, A. Russman, G. Majmudar, R. Singer, T. Hamilton, J. Voorhees, Restoration of collagen formation in photodamaged human skin by tretinoin (retinoic acid), N. Engl. J. Med. 327 (1993) 669–677, https://doi.org/10.1056/NEJM199209033271001.
[21] Z. Qin, J.J. Voorhees, G.J. Fisher, T. Quan, Age-associated reduction of cellular spreading/mechanical force up-regulates matrix metalloproteinase-1 expression and collagen fibril fragmentation via c-Jun/AP-1 in human dermal fibroblasts, Aging Cell 13 (2014) 1028–1037, https://doi.org/10.1111/acel.12265.
[22] J.S. Bredfeldt, C.A. Pehlke, M.W. Conklin, J.M. Szulczewski, D.R. Inman, P.J. Keely, R.D. Nowak, T.R. Mackie, K.W. Eliceiri, Computational segmentation of collagen fibers from second-harmonic generation images of breast cancer, J. Biomed. Opt. 19 (2014) 1–10, https://doi.org/10.1117/1.JBO.19.1.016007.
[23] Z. Wang, M. Boudjelal, S. Kang, J.J. Voorhees, G.J. Fisher, Ultraviolet irradiation of human skin causes functional vitamin A deficiency, preventable by all-trans retinoic acid pretreatment, Nat. Med. 5 (1999) 418–422, https://doi.org/10.1038/7417.
[24] A.S. Barrett, M.J. Wither, R.C. Hill, M. Dzieciatkowska, A. D'Alessandro, J.A. Reisz, K.C. Hansen, Hydroxylamine chemical digestion for insoluble extracellular matrix characterization, J. Proteome Res. 44 (2017) 319–335, https://doi.org/10.1111/cdoe.12200.
[25] J.R. Wiśniewski, A. Zougman, N. Nagaraj, M. Mann, Universal sample preparation method for proteome analysis, Nat. Methods 6 (2009) 359–362, https://doi.org/10.1038/nmeth.1322.
[26] R.J. Beynon, M.K. Doherty, J.M. Pratt, S.J. Gaskell, Multiplexed absolute quantification in proteomics using artificial QCAT proteins of concatenated signature peptides, Nat. Methods 2 (2005) 587–589, https://doi.org/10.1038/nmeth774.
[27] T.D. Johnson, R.C. Hill, M. Dzieciatkowska, V. Nigam, A. Behfar, K.L. Christman, K.C. Hansen, Quantification of decellularized human myocardial matrix: a comparison of six patients, Proteomics Clin. Appl. 10 (2016) 75–83, https://doi.org/10.1002/prca.201500048.
[28] R.C. Hill, E.A. Calle, M. Dzieciatkowska, L.E. Niklason, K.C. Hansen, Quantification of extracellular matrix proteins from a rat lung scaffold to provide a molecular readout for tissue engineering, Mol. Cell. Proteomics 14 (2015) 961–973, https://doi.org/10.1074/mcp.M114.045260.
[29] B. MacLean, D.M. Tomazela, N. Shulman, M. Chambers, G. L. Finney, B. Frewen, R. Kern, D.L. Tabb, D.C. Liebler, M.J. MacCoss, Skyline: an open source document editor for creating and analyzing targeted proteomics experiments, Bioinformatics. 26 (2010) 966–968, https://doi.org/10.1093/bioinformatics/btq054.
[30] E.T. Goddard, R.C. Hill, A. Barrett, C. Betts, Q. Guo, O. Maller, V.F. Borges, K.C. Hansen, P. Schedin, Quantitative extracellular matrix proteomics to study mammary and liver tissue microenvironments, Int. J. Biochem. Cell Biol. 81 (2016) 223–232, https://doi.org/10.1161/CIRCULATIONAHA.115.017472.
[31] S. Tyanova, T. Temu, P. Sinitcyn, A. Carlson, M.Y. Hein, T. Geiger, M. Mann, J. Cox, The Perseus computational platform for comprehensive analysis of (prote) omics data, Nat. Methods 13 (2016) 731–740, https://doi.org/10.1038/nmeth.3901.
[32] E.I. Boyle, S. Weng, J. Gollub, H. Jin, D. Botstein, M.J. Cherry, G. Sherlock, GO::TermFinder—open source software for accessing Gene Ontology information and finding significantly enriched Gene Ontology terms associated with a list of genes, Bioinformatics. 20 (2004) 3710–3715, https://doi.org/10.1093/bioinformatics/bth456.
[33] A. Gautieri, A. Redaelli, M.J. Buehler, S. Vesentini, Age- and diabetes-related nonenzymatic crosslinks in collagen fibrils: candidate amino acids involved in Advanced Glycation End-products, Matrix Biol. 34 (2014) 89–95, https://doi.org/10.1016/j.matbio.2013.09.004.
[34] M. Yamauchi, D.T. Woodley, G.L. Mechanic, Aging and cross-linking of skin collagen, Biochem. Biophys. Res. Commun. 152 (1988) 898–903.
[35] M. Murakami, T. Kambe, S. Shimbara, I. Kudo, Functional coupling between various phospholipase A2s and cyclooxygenases in immediate and delayed prostanoid biosynthetic pathways, J. Biol. Chem. 274 (1999) 3103–3115.
[36] M. Giesen, S. Gruedl, O. Holtkoetter, G. Fuhrmann, A. Koerner, D. Petersohn, Ageing processes influence keratin and KAP expression in human hair follicles, Exp. Dermatol. 20 (2011) 749–775, https://doi.org/10.1111/j.1600-0625.2011.01301.x.

[37] S. Zhuo, X. Zhu, J. Chen, S. Xie, Quantitative biomarkers of human skin photoaging based on intrinsic second harmonic generation signal, Scanning. 35 (2013) 273–276, https://doi.org/10.1002/sca.21062.
[38] E. Janig, M. Haslbeck, A. Aigelsreiter, N. Braun, D. Unterthor, P. Wolf, N.M. Khaskhely, J. Buchner, H. Denk, K. Zatloukal, Clusterin associates with altered elastic fibers in human photoaged skin and prevents elastin from ultraviolet-induced aggregation in vitro, Am. J. Pathol. 171 (2007) 1474–1482, https://doi.org/10.2353/ajpath.2007.061064.
[39] L. Rittié, B. Perbal, J.J. Castellot, J.S. Orringer, J.J. Voorhees, G.J. Fisher, Spatial-temporal modulation of CCN proteins during wound healing in human skin in vivo, J. Cell Commun. Signal. 5 (2011) 69–80, https://doi.org/10.1007/s12079-010-0114-y.
[40] H. Xu, P. Li, M. Liu, C. Liu, Z. Sun, X. Guo, Y. Zhang, CCN2 and CCN5 exerts opposing effect on fibroblast proliferation and transdifferentiation induced by TGF-β, Clin. Exp. Pharmacol. Physiol. 42 (2015) 1207–1219, https://doi.org/10.1111/1440-1681.12470.
[41] G.J. Fisher, T. Quan, T. Purohit, J. Varani, S. Kang, J.J. Voorhees, Collagen fragmentation promotes oxidative stress and elevates matrix metalloproteinase-1 in fibroblasts in aged human skin, Am. J. Pathol. 174 (2009) 101–114, https://doi.org/10.2353/ajpath.2009.080599.
[42] J.Y. Seo, S.H. Lee, C.S. Youn, H.R. Choi, G. Rhie, K.H. Cho, K.H. Kim, K.C. Park, H.C. Eun, J.H. Chung, Ultraviolet radiation increases tropoelastin mRNA expression in the epidermis of human skin in vivo, J. Invest. Dermatol. 116 (2001) 915–919, https://doi.org/10.1046/j.1523-1747.2001.01358.x.
[43] Z. Chen, J.Y. Seo, Y.K. Kim, S.R. Lee, K.H. Kim, K.H. Cho, H. C. Eun, J.H. Chung, Heat modulation of tropoelastin, fibrillin-1, and matrix metalloproteinase-12 in human skin in vivo, J. Invest. Dermatol. 124 (2005) 70–78, https://doi.org/10.1111/j.0022-202X.2004.23550.x.
[44] H.Y. Chang, J.T. Chi, S. Dudoit, C. Bondre, M. Van De Rijn, D. Botstein, P.O. Brown, Diversity, topographic differentiation, and positional memory in human fibroblasts, Proc. Natl. Acad. Sci. U. S. A. 99 (2002) 12877–12882, https://doi.org/10.1073/pnas.162488599.
[45] D. Kiritsi, C. Has, L. Bruckner-tuderman, Laminin 332 in junctional epidermolysis bullosa, Cell Adhes. Migr. 7 (2013) 135–141.
[46] T. Kainulainen, L. Häkkinen, S. Hamidi, K. Larjava, M. Kallioinen, J. Peltonen, T. Salo, H. Larjava, A. Oikarinen, Laminin-5 expression is independent of the injury and the microenvironment during reepithelialization of wounds, J. Histochem. Cytochem. 46 (1998) 353–360.
[47] R.F. Ghohestani, K. Li, P. Rousselle, J. Uitto, Molecular organization of the cutaneous basement membrane zone, Clin. Dermatol. 19 (2001) 551–562.
[48] S. Amano, Possible involvement of basement membrane damage in skin photoaging, J. Investig. Dermatology Symp. Proc. 14 (2009) 2–7, https://doi.org/10.1038/jidsymp.2009.5.
[49] F. Vazquez, S. Palacios, N. Aleman, F. Guerrero, Changes of the basement membrane and type IV collagen in human skin during aging, Maturitas. 25 (1996) 209–215, https://doi.org/10.1016/S0378-5122(96)01066-3.
[50] J. Tigges, J. Krutmann, E. Fritsche, J. Haendeler, H. Schaal, J.W. Fischer, F. Kalfalah, H. Reinke, G. Reifenberger, K. Stühler, N. Ventura, S. Gundermann, P. Boukamp, F. Boege, The hallmarks of fibroblast ageing, Mech. Ageing Dev. 138 (2014) 26–44, https://doi.org/10.1016/j.mad.2014.03.004.
[51] S. Bakerman, Quantitative extraction of acid-soluble human skin collagen with age, Nature 196 (1962).
[52] N. Basisty, A. Kale, O.H. Jeon, C. Kuehnemann, T. Payne, C. Rao, A. Holtz, S. Shah, V. Sharma, L. Ferrucci, J. Campisi, B. Schilling, A proteomic atlas of senescence-associated secretomes for aging biomarker development, PLoS Biol. 18 (2020), e3000599. https://doi.org/10.1371/journal.pbio.3000599.
[53] S.M.N.A. Hafez, Age related changes in the dermal mast cells and the associated changes in the dermal collagen and cells: a histological and electron microscopy study, Acta Histochem. (2019)https://doi.org/10.1016/j.acthis.2019.05.004.
[54] J. Uitto, Biochemistry of the elastic fibers in normal connective tissues and its alterations in diseases, J. Invest. Dermatol. 72 (1979) 1–10.
[55] B.S.M. Mithieux, A.S. Weiss, Elastin 70 (2006) 437–461, https://doi.org/10.1016/S0065-3233(04)70013-3.
[56] F. Sato, R. Seino-sudo, M. Okada, H. Sakai, T. Yumoto, H. Wachi, Lysyl oxidase enhances the deposition of tropoelastin through the catalysis of tropoelastin molecules on the cell surface, Biol. Pharm. Bull. 40 (2017) 1646–1653.
[57] E. Noblesse, V. Cenizo, C. Bouez, A. Borel, C. Gleyzal, S. Peyrol, M.P. Jacob, P. Sommer, O. Damour, Lysyl oxidase-like and lysyl oxidase are present in the dermis and epidermis of a skin equivalent and in human skin and are associated to elastic fibers, J. Invest. Dermatol. 122 (2004) 621–630, https://doi.org/10.1111/j.0022-202X.2004.22330.x.
[58] T. Nakamura, P.R. Lozano, Y. Ikeda, Y. Iwanaga, A. Hinek, S. Minamisawa, C.-F. Cheng, K. Kobuke, N. Dalton, Y. Takada, K. Tashirok, J.R. Jr, T. Honjo, K.R. Chien, Fibulin-5/DANCE is essential for elastogenesis in vivo, Nature. 415 (2002) 171–175.
[59] Z. Chen, M.H. Shin, Y.J. Moon, S.R. Lee, Y.K. Kim, J.E. Seo, J.E. Kim, K.H. Kim, J.H. Chung, Modulation of elastin exon 26A mRNA and protein expression in human skin in vivo, Exp. Dermatol. 18 (2009) 378–386, https://doi.org/10.1111/j.1600-0625.2008.00799.x.
[60] S. Chakravarti, Functions of lumican and fibromodulin: lessons from knockout mice, Glycoconj. J. 19 (2002) 287–293, https://doi.org/10.1023/A:1025348417078.
[61] C. Ruhland, E. Schonherr, H. Robenek, U. Hansen, R.V. Iozzo, P. Bruckner, D.G. Seidler, The glycosaminoglycan chain of decorin plays an important role in collagen fibril formation at the early stages of fibrillogenesis, FEBS J. 274 (2007) 4246–4255, https://doi.org/10.1111/j.1742-4658.2007.05951.x.
[62] K.A. Robinson, M. Sun, C.E. Barnum, S.N. Weiss, J. Huegel, S.S. Shetyea, L. Linb, D. Saezb, S.M. Adamsb, R.V. Iozzoc, L.J. Soslowskya, D.E. Birk, Decorin and biglycan are necessary for maintaining collagen fibril structure, fiber realignment, and mechanical properties of mature tendons, Matrix Biol. 64 (2017) 81–93, https://doi.org/10.1016/j.matbio.2017.08.004.
[63] E.S. Tasheva, A. Koester, A.Q. Paulsen, A.S. Garrett, D.L. Boyle, H.J. Davidson, M. Song, N. Fox, G.W. Conrad, Mimecan/osteoglycin-deficient mice have collagen fibril abnormalities, Mol. Vis. 8 (2002) 407–415 (https://doi.org/v8/a48, pii).
[64] K. Stuart, J. Paderi, P.W. Snyder, L. Freeman, A. Panitch, Collagen-binding peptidoglycans inhibit MMP mediated collagen degradation and reduce dermal scarring, 6 (2011) https://doi.org/10.1371/journal.pone.0022139.
[65] H.M. Kagan, W. Li, Lysyl oxidase: properties, specificity, and biological roles inside and outside of the cell, J. Cell. Biochem. 88 (2003) 660–672, https://doi.org/10.1002/jcb.10413.
[66] D. Quaglln, C. Fornieri, L.B. Nanney, J.M. Davidson, Extracellular matrix modifications in rat tissues of different

ages: correlations between elastin and collagen type I mRNA expression and lysyl-oxidase activity, Matrix Collagen Relat. Res. 13 (1993) 481–490, https://doi.org/10.1016/S0934-8832(11)80114-9.

[67] V. Cenizo, V. Andre, C. Reymermier, P. Sommer, O. Damour, E. Perrier, LOXL as a target to increase the elastin content in adult skin: a dill extract induces the LOXL gene expression, Exp. Dermatol. (2006) 574–581, https://doi.org/10.1111/j.0906-6705.2006.00442.x.

[68] D. Aeschlimann, V. Thomazy, Protein crosslinking in assembly and remodelling of extracellular matrices: the role of transglutaminases, Connect. Tissue Res. 8207 (2009) https://doi.org/10.3109/03008200009005638.

[69] V. Frezza, A. Terrinoni, C. Pitolli, A. Mauriello, G. Melino, E. Candi, Transglutaminase 3 protects against photodamage, J. Invest. Dermatol. 137 (2017) 1590–1594, https://doi.org/10.1016/j.jid.2017.02.982.

[70] T.E. Cawston, D.A. Young, Proteinases involved in matrix turnover during cartilage and bone breakdown, Cell Tissue Res. 339 (2010) 221–235, https://doi.org/10.1007/s00441-009-0887-6.

[71] W. Hornebeck, Down-regulation of tissue inhibitor of matrix metalloprotease-1 (TIMP-1) in aged human skin contributes to matrix degradation and impaired cell growth and survival, Pathol. Biol. 51 (2003) 569–573, https://doi.org/10.1016/j.patbio.2003.09.003.

[72] G. Fassina, N. Ferrari, C. Brigati, R. Benelli, L. Santi, D.M. Noonan, A. Albini, P. Neoplastica, I. Nazionale, C. Neurofisiologia, Tissue inhibitors of metalloproteases: regulation and biological activities, Clin. Exp. Metastasis. 18 (2000) 111–120.

[73] A.M. Macgregor, C.G. Eberhart, M. Fraig, J. Lu, M.K. Halushka, Tissue inhibitor of matrix metalloproteinase-3 levels in the extracellular matrix of lung, kidney, and eye increase with age, J. Histochem. Cytochem. 57 (2009) 207–213, https://doi.org/10.1369/jhc.2008.952531.

[74] M.R. Buck, D.G. Karustis, N.A. Day, K.V. Honntt, B.F. Sloane, Degradation of extracellular-matrix proteins by human cathepsin B from normal and tumour tissues, Biochem J. 282 (1992) 273–278.

[75] R.A. Maciewicz, S.F. Wotton, D.J. Etherington, V.C. Duance, Susceptibility of the cartilage collagens types II, IX and XI to degradation by the cysteine proteinases, cathepsins B and L, FEBS Lett. 269 (1990) 189–193.

[76] H. Bu, P. Luigi, R. Ostafe, M. Rehders, R. Dannenmann, N. Schaschke, P. Boukamp, Cathepsin B is essential for regeneration of scratch-wounded normal human epidermal keratinocytes, 86 (2007) 747–761, https://doi.org/10.1016/j.ejcb.2007.03.009.

[77] J. Sage, D. De Quéral, E. Leblanc-noblesse, R. Kurfurst, S. Schnebert, E. Perrier, C. Nizard, G. Lalmanach, F. Lecaille, Differential expression of cathepsins K, S and V between young and aged Caucasian women skin epidermis, Matrix Biol. 33 (2014) 41–46, https://doi.org/10.1016/j.matbio.2013.07.002.

[78] Y. Zheng, W. Lai, M. Wan, H.I. Maibach, Expression of cathepsins in human skin, Skin Pharmacol. Physiol. 24 (2011) 10–21, https://doi.org/10.1159/000314725.

[79] S.D. Lamore, G.T. Wondrak, UVA causes dual inactivation of cathepsin B and L underlying lysosomal dysfunction in human dermal fibroblasts, J. Photochem. Photobiol. B 123 (2013) 1–12, https://doi.org/10.1016/j.jphotobiol.2013.03.007.

[80] L. Wei, Z. Yue, Y. Zhang-zhang, S. Xiang-yang, W. Miao-jian, G. Zi-jian, X. Xiao-yuan, L. Wei, Changes of cathepsin B in human photoaging skin both in vivo and in vitro, Chin. Med. J. 123 (2010) 527–531, https://doi.org/10.3760/cma.j.issn.0366-6999.2010.05.004.

[81] Y. Zheng, H. Chen, W. Lai, Q. Xu, C. Liu, L. Wu, H.I. Maibach, Cathepsin D repairing role in photodamaged skin barrier, Skin Pharmacol. Physiol. (2014)https://doi.org/10.1159/000363248.

[82] E. An, S. Sen, S.K. Park, H. Gordish-dressman, Y. Hathout, Identification of novel substrates for the serine protease HTRA1 in the human RPE secretome, Integr. Opthalmology Vis. Sci. 51 (2010) 3379–3386, https://doi.org/10.1167/iovs.09-4853.

[83] J.R. Graham, A. Chamberland, Q. Lin, X.J. Li, D. Dai, W. Zeng, M.S. Flannery, Carl Ryan, M.A. Rivera-Bermudez, Z. Yang, Serine protease HTRA1 antagonizes transforming growth factor-B signaling by cleaving its receptors and loss of HTRA1 in vivo enhances bone formation, PLoS One 8 (2013) 1–8, https://doi.org/10.1371/journal.pone.0074094.

[84] C. Oka, R. Tsujimoto, M. Kajikawa, K. Koshiba-takeuchi, J. Ina, M. Yano, A. Tsuchiya, Y. Ueta, A. Soma, H. Kanda, M. Matsumoto, M. Kawaichi, Htr A1 serine protease inhibits signaling mediated by Tgf-β family proteins, Development. 131 (2004) 1041–1053, https://doi.org/10.1242/dev.00999.

[85] M.O. Li, Y.Y. Wan, S. Sanjabi, A.-K.L. Robertson, R.A. Flavell, Transforming growth factor-β regulation of immune responses, Annu. Rev. Immunol. 24 (2006) 99–146, https://doi.org/10.1146/annurev.immunol.24.021605.090737.